Applied Physics Letters

Planar lighting from optimized graphite papers made of graphite oxide

Cite as: Appl. Phys. Lett. **110**, 211903 (2017); https://doi.org/10.1063/1.4984132
Submitted: 25 February 2017 . Accepted: 08 May 2017 . Published Online: 24 May 2017

Ziqi Tan, Huailiang Xu, Bucun Zhou, Zeming Qi, Yan Qu, and Yanwu Zhu

View Online Export Citation CrossMark

ARTICLES YOU MAY BE INTERESTED IN

Dispersive readout of a silicon quantum dot with an accumulation-mode gate sensor
Applied Physics Letters **110**, 212101 (2017); https://doi.org/10.1063/1.4984224

Composition dependent phase transition and its induced hysteretic effect in the thermal conductivity of $W_xMo_{1-x}Te_2$
Applied Physics Letters **110**, 211904 (2017); https://doi.org/10.1063/1.4984143

Prospective for graphene based thermal mid-infrared light emitting devices
AIP Advances **4**, 087139 (2014); https://doi.org/10.1063/1.4894449

Challenge us.
What are your needs for periodic signal detection?
Watch

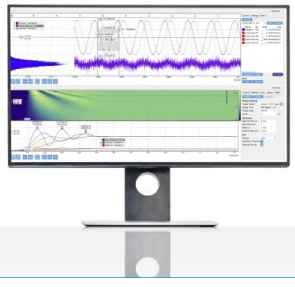

Zurich Instruments

AIP Publishing

© 2017 Author(s).

Planar lighting from optimized graphite papers made of graphite oxide

Ziqi Tan,[1] Huailiang Xu,[2] Bucun Zhou,[3] Zeming Qi,[4] Yan Qu,[2] and Yanwu Zhu[1]
[1]*Key Laboratory of Materials for Energy Conversion, Chinese Academy of Sciences, Department of Materials Science and Engineering, i-ChEM, University of Science and Technology of China, 96 Jin Zhai Rd., Hefei, Anhui 230026, People's Republic of China*
[2]*The Sixth Element (Changzhou) Materials Technology Co., Ltd., 9 West Tai Lake Avenue, Changzhou, Jiangsu 213000, People's Republic of China*
[3]*Changzhou Fuxi Technology Co., Ltd., 5 Industrial Road, Changzhou, Jiangsu 213144, People's Republic of China*
[4]*National Synchrotron Radiation Laboratory, University of Science and Technology of China, 96 Jin Zhai Rd., Hefei, Anhui 230026, People's Republic of China*

(Received 25 February 2017; accepted 8 May 2017; published online 24 May 2017)

We report the preparation of large-area graphite papers with thicknesses from 100 μm to more than 1 mm, by the reduction and graphitization of graphite oxide at elevated temperatures. The papers can be produced on a size of $20 \times 20\,cm^2$ and have a low mass density. X-ray diffraction and Raman characterization show that the stacking of graphitic layers in the papers follows the Bernal stacking, and X-ray photoelectron spectroscopy indicates a carbon purity of above 98 at. % in the papers. The graphite papers have an electrical conductivity of 2533–4996 S/m and a thermal conductivity of 42–149 W/mK, depending on the thickness. When a power input of above 10 W is applied on the paper with a thickness of 98 μm, incandescence is observed, corresponding to a temperature of higher than 1000 °C, which is increased with the input power. *Published by AIP Publishing.* [http://dx.doi.org/10.1063/1.4984132]

Graphitic carbons have high melting temperatures and high sublimation temperatures of above ~3700 K in vacuum,[1] which can be utilized in electroluminescent cells. The use of graphitic carbons for incandescence can be dated back to Edison's first commercial light bulb in which carbonized bamboo was used.[2] The Stefan-Boltzmann law indicates that the radiation output of a black body scales as T,[4] suggesting that a higher temperature allows more radiation in the visible range; thus, a graphitic carbon incandescent source could operate at high temperatures and tolerate high input powers.[2] With outstanding electrical conductivity and excellent chemical stability, graphene is able to carry a large current of up to $10^8\,A/cm^2$,[3] which makes graphene a promising incandescent source.[4] Biswas *et al.* reported a radiation of mid-infrared light from $0.5 \times 0.5\,mm^2$ graphene made by chemical vapor deposition (CVD) and transferred onto a SiO_2/Si substrate; the radiation corresponds to a grey-body emitter, with emissivity values of approximately 2% and 6% for mono- and multilayer graphene, which were calculated by comparing the difference in measured intensities using a blackbody calibrator.[5] On the other hand, the macroscopic assembly of graphene platelets made from graphite oxide (GO)[6–8] has been developed as incandescent radiation sources. For example, Yu and Dai reported stable, bright, and uniform incandescent emission from $0.5 \times 1.0\,cm^2$ graphene films (with a thickness of 1.2 nm) fabricated by vacuum filtration and thermal treatment of chemically reduced graphene oxide dispersion (by exfoliation of GO), in which both turn-on voltage (~6 V) and demanding vacuum (0.05 Torr) were lower than those required for carbon nanotubes and conventional tungsten filaments.[9] Bao *et al.* prepared a highly conducting carbon paper (thickness 0.5–1 μm) composed of graphene oxide platelets interpenetrated with 10 wt. % single walled carbon nanotubes, which demonstrated compelling lighting performance and sustained a temperature of about 3000 K.[2] However, no graphite papers with macroscopic thicknesses (hundred μm to mm) have been investigated as incandescent radiation sources.

In this work, we report the production of large-area graphite papers with tunable thicknesses from about 100 μm to above 1000 μm in a size of as large as $20 \times 20\,cm^2$ and their incandescent emission performance. Befitting to the high carbon purity, excellent electric conductivity, and reasonable thermal conductivity, the graphite papers emit candescence in a vacuum chamber for an input power of about 10 W. The graphite paper with a thickness of 98 μm and an area of $2 \times 30\,mm^2$ shows incandescence with the black-body radiation temperature of 1876 K for an input power of 41.0 W.

In the typical preparation, GO was prepared by modified Hummers' method.[10] GO slurry (20 mg/ml) made by the high speed stirring of GO in deionized water was coated on a polyethylene terephthalate substrate and dried at 60 °C in ambiance to form films. The dried GO films were pre-annealed at 1000 °C to reduce GO and further annealed at 2800 °C for 2 h in an argon atmosphere to prepare the final graphite papers. The dried GO films have a typical thickness of ~100 μm, and the graphite papers were made by stacking various numbers of dried GO films before annealing. By changing the numbers of stacked dried GO films, three graphite papers were prepared, with thicknesses of 98 ± 10 μm, 347 ± 37 μm, and 1153 ± 70 μm and thus named S98, S347, and S1153, respectively. The coating area and the coating thickness of GO can be tuned to tailor the size and the thickness of graphite papers obtained. The morphology and the structure of samples were characterized by scanning electron microscopy (SEM, JSM-6700F),

transmission electron microscopy (TEM, JEOL 2010), X-ray diffraction (XRD, D/max-TTR III) with Cu K_α radiation ($V = 40\,kV$, $I = 200\,mA$), and Raman spectroscopy (Renishaw in Via Raman Microscope, 532 nm laser, 5 mW). X-ray photoelectron spectroscopy (XPS, ESCALAB 250) and thermogravimetric analysis (TGA, TGA Q5000IR) were used to analyze the chemical components. The mechanical properties, thermal transport, and electrical conductivity of samples were characterized using dynamic thermomechanical analysis (DMA, Q800), Laser flash diffusivity apparatus (LFA 467), and an electrochemical station (PARSTAT 4000, Princeton Applied Research), respectively. To investigate the incandescent behavior, graphite papers were cut into a belt shape with a length of 2–5 mm and suspended between two copper electrodes which were connected to a power supply. The device was then placed in a vacuum chamber with a pressure of 0.1–1 Pa for incandescent collection by an optical fiber. The spectrum of emission was then detected using a spectrometer (NOVA, Ideaoptics Technology Ltd.) at room temperature. For the spectral measurement, the spectrometer including an optical fiber was first calibrated with a National Institute for Standards and Technology (NIST)-traceable light source for calibrating the radiance as a function of wavelength. The radiant flux density versus wavelength curves was obtained by normalizing raw data with the standard light source.

Figure 1(a) shows the surface morphology of the graphite paper with a thickness of 98 μm, and the wrinkles are clearly observed. The inset shows a S98 graphite paper with a size of $20 \times 20\,cm^2$. In Fig. 1(b), the cross-section of paper with a thickness of 98 μm is shown, indicating a layer-by-layer stacking in the paper while accompanying a large interlayer space and disordered orientations. The graphite paper is freestanding and flexible; a bending by tweezers is demonstrated in Fig. 1(c). The TEM image [Fig. 1(d)] of the graphite paper of 98 μm shows that the paper consists of graphitic platelets, and a typical interlayer distance of 0.35 nm [inset in Fig. 1(d)] is identified, slightly larger than the interlayer space of graphite.[11] The apparent density of graphite papers has been measured to be $0.24\,g/cm^3$, $0.18\,g/cm^3$, and $0.17\,g/cm^3$ for S98, S347, and S1153, respectively, much lower than $2.26\,g/cm^3$ in graphite. Such a density is likely caused by the large space in the graphitic layers, generated by the expansion during the thermal annealing of GO films.[12]

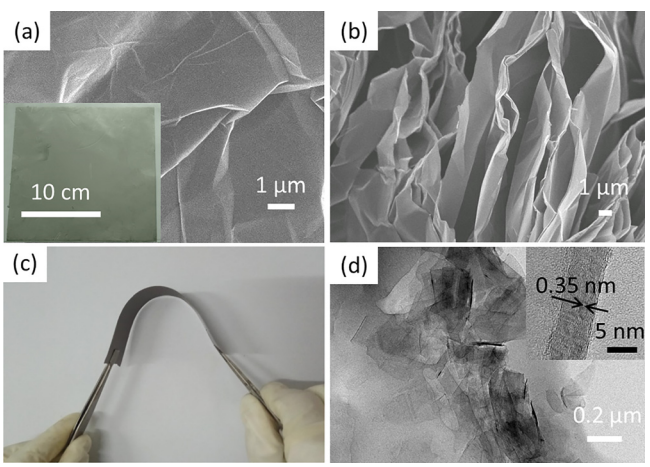

FIG. 1. (a) SEM image of the surface of S98. Inset: digital image of S98. (b) SEM image of the cross-section of S98. (c) Photograph of a bended graphite paper. (d) TEM image of S98, and the inset shows a high resolution TEM image of S98.

The XRD data shown in Fig. 2(a) reveal two typical peaks corresponding to (002) and (004) planes in graphite. An interlayer spacing of 0.34 nm has been calculated from the (002) peak using the Bragg formula, close to that in graphite.[11] However, other characteristic diffraction peaks of graphite, e.g., the peaks of (100) and (110) diffraction peaks,[13] are not observed in the XRD patterns of graphite papers, which could be explained by the partial exfoliation of graphite papers and the corrugated graphitic platelets in the papers as observed in TEM [Fig. 1(d)].[14] Raman spectra shown in Fig. 2(b) confirm the nearly complete recovery of the conjugated graphitic structure in the graphite papers. The D peak ($1350\,cm^{-1}$) is absent in all spectra, revealing the low topological defect concentrations of graphite papers. The G ($1582\,cm^{-1}$), D + D″ ($2450\,cm^{-1}$), and 2D ($2716\,cm^{-1}$) peaks are similar to those in graphite.[15] The asymmetry of the 2D peak is a clear indication of Bernal stacking.[16] In the XPS spectra shown in Fig. 2(c), the C 1 s (285 eV) peaks can be seen as the typical feature of sp^2 carbon with the monopole-like electron transition between the HOMO-LUMO gap and the dipole like $\pi \rightarrow \pi^*$ shake-up feature;[17] a weak O 1 s (533 eV) peak due to oxygen-containing groups exists as well. As the thickness increases, the oxygen content decreases from 1.90 at. % for S98 to 1.38 at. % for S347 and 0.38 at. % for S1153. The thermogravimetric analysis (TGA) [Fig. 2(d)] of graphite papers has shown the thermal stability in air till 800 °C. As there is no sharp weight loss at lower temperatures for graphite papers, most oxygen-containing groups have been removed by the calcination process.

The mechanical properties of graphite papers have been investigated by tensile tests, as shown in Fig. 3(a). From the enlarged view of the stress-strain curves in the low strain range,[18] the Young's modulus is calculated to be 193.6 MPa, 118.3 MPa, and 78.6 MPa for S98, S347, and S1153,

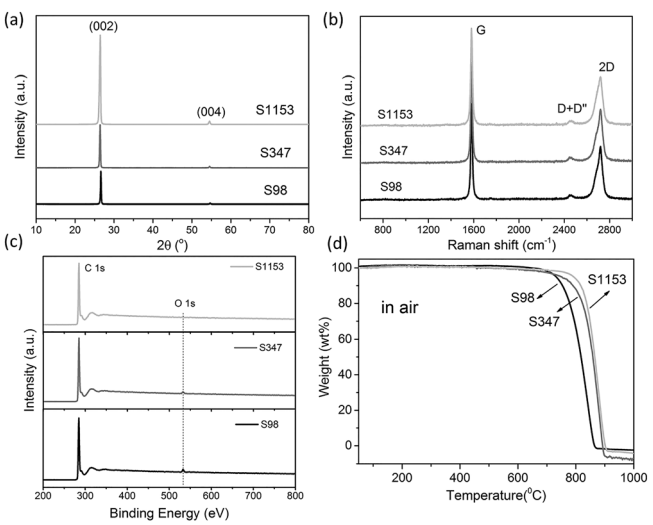

FIG. 2. (a) XRD patterns, (b) Raman spectra, (c) XPS spectra of S98, S347, and S1153, and (d) TGA curves of graphite papers.

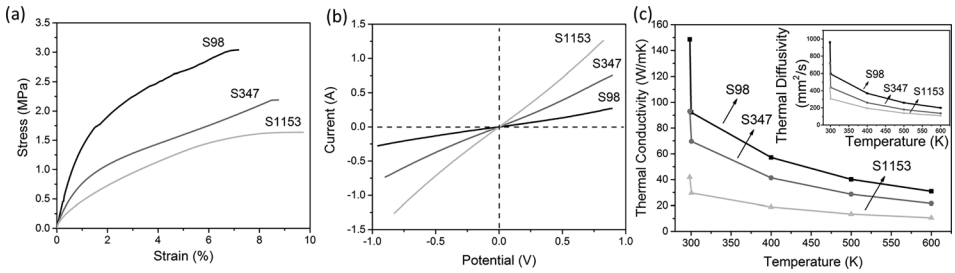

FIG. 3. (a) Tensile stress-strain curves for all graphite papers. (b) Current vs voltage curves of all graphite papers with the same length of 21 mm and the same width of 11 mm. (c) Thermal conductivity of all graphite papers (inset: thermal diffusivity).

respectively. These values are much lower than those of graphene (~1 TPa).[6] The breaking strength of S98, S347, and S1153 is 3.0 MPa, 2.2 MPa, and 1.6 MPa. Presumably, when the GO papers are heated, a release of gaseous species (e.g., CO_2, CO, and H_2O) and a large amount of crumples may have led to a sponge-like structure and thus the low density and low mechanical strength, due to the reduced mechanical integrity.[19] Figure 3(b) shows the current voltage curves of samples with the same size of $11 \times 21\,mm^2$, from which the electrical conductivity of 4996 S/m, 4096 S/m, and 2353 S/m was obtained for S98, S347, and S1153, respectively. The electrical conductivities of graphite papers are much higher than those of graphene films with thicknesses of nanometers as well (e.g., ~1700 S/m)[20] due to the conjugated graphitic structure. The thermal conductivity [Fig. 3(c)] is obtained to be 148.6 W/mK, 92.9 W/mK, and 42.0 W/mK for S98, S347, and S1153, respectively, measured at room temperature (298 K). The thermal diffusivities [inset of Fig. 3(c)] of S98, S347, and S1153 are measured to be $960.7\,mm^2/s$, $714.5\,mm^2/s$, and $433.1\,mm^2/s$. The thermal conductivity of graphite paper is much lower than the value of 2000 W/mK for in-plane graphene.[21] However, the low thermal conductivity of graphite papers may benefit to the radiative efficiency in electroluminescent materials.[2]

When a current passes through a ribbon cut from a graphite paper, the majority of Joule heating is dissipated as radiation, which can be readily observed by the eye and detected using a spectrometer. Figures 4(a) and 4(b) show images taken on a S98 ribbon with a size of $2 \times 30\,mm^2$ with different currents. When the input power is increased to above 10 W, the ribbon starts to illuminate from the central part, as shown in Fig. 4(a). As the power increases to 58 W, a strong radiation is observed across the whole ribbon as shown in Fig. 4(b). The emission at the 'hot-spot' is approximately half-way between the source and the drain contacts as shown in Fig. 4(a), indicating a Joule heating mechanism of the graphite paper.[5]

For the blackbody irradiation model, the radiation can be described by the Planck function

$$B_\lambda(\lambda, T) = \gamma \frac{2hc^2}{\lambda^5} \frac{1}{e^{hc/\lambda k_B T} - 1},$$

where k_B is the Boltzmann constant, h the Planck constant, and c the speed of light, and the scaling constant γ is introduced to allow for the unknown but constant geometric view factor between the ribbon and the optical fiber. By fitting the curves of radiance intensity versus wavelength with Planck's law, the temperature values were obtained and are shown in Fig. 4(d) for S98 and S347 with different sizes. For the 2-mm-wide S98 ribbon, the temperature estimated is increased from 1319 to 1876 K, as the input power is increased from 11.3 to 41.0 W. By comparing the values for four similar devices with different thicknesses and widths (all with the same length), we can see that thicker graphite papers need higher input powers to reach the same temperature, while the smaller width benefits to the high incandescent temperature for the same thickness and input power. The S1153 paper did not show incandescence in the power range of the power supply.

The conversion efficiency from electricity into radiation can be estimated using the expression $\eta_{\text{electricity}\to\text{radiation}} = 1 - \frac{\tanh(L\sqrt{2h_{rad}/\sqrt{kt}})}{L\sqrt{2h_{rad}/\sqrt{kt}}}$. Among the parameters, h_{rad} is the radiative heat transfer coefficient,[2] L is the length of the sample, t is the thickness of the sample, and k is the in-plane thermal conductivity. According to the expression, devices that are long and thin while with low-k are the best at converting electrical power into radiation, which leads to higher temperature. The graphite paper ribbons in this work have the same length while different thermal conductivities all below 50 W/mK at high temperatures. Thus, S98 with a width of 2 mm shows the best light emission behavior.

In summary, we have fabricated graphite paper samples with a size of as large as $20 \times 20\,cm^2$, with a thickness of between hundred micrometers and millimeters. The graphite papers have high thermal stability, good electronic conductivity, and suitable thermal conductivity. We have found that the

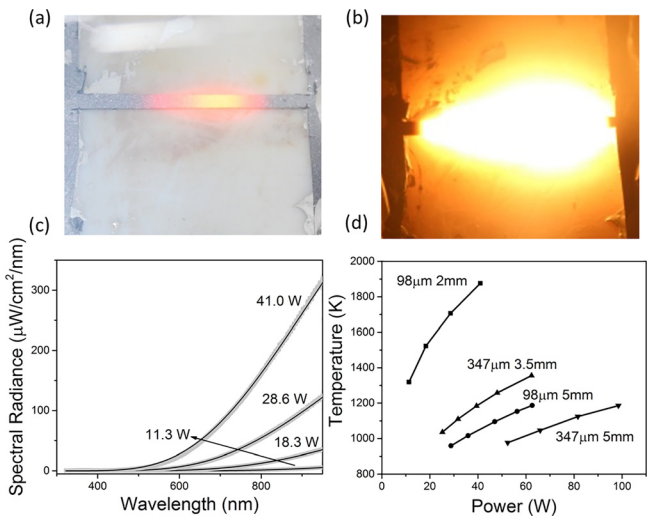

FIG. 4. Digital photos of incandescence of a ribbon of S98 (size: $2 \times 30\,mm^2$) with applied electrical powers of (a) 10 W and (b) 58 W. (c) Radiance spectral measurement of the S98 sample with increased electrical power inputs. Solid black curves show the fitting of the spectra with Planck's law by assuming a constant emissivity. (d) Fitted temperature versus input electrical power for four graphite paper samples with a similar geometry (S98: $2 \times 30\,mm^2$ and $5 \times 30\,mm^2$; S347: $3.5 \times 30\,mm^2$ and $5 \times 30\,mm^2$).

graphite paper samples with thicknesses of 98 and 347 μm have incandescence upon sufficient applied power, which can be used to provide solutions for lighting/heating needs.

We acknowledge financial support from the China Government 1000 Plan Talent Program, the China MOE NCET Program, the Natural Science Foundation of China (51322204), the Fundamental Research Funds for the Central Universities (WK2060140014 and WK2060140017), and the Technological Development Grant of Hefei Science Center of CAS (2014TDG-HSC002).

[1]A. G. Whittaker, Nature **276**(5689), 695–696 (1978).
[2]W. Bao, A. D. Pickel, Q. Zhang, Y. Chen, Y. Yao, J. Wan, K. K. Fu, Y. Wang, J. Dai, H. Zhu, D. Drew, M. Fuhrer, C. Dames, and L. Hu, Adv. Mater. **28**(23), 4684–4691 (2016).
[3]J. Yu, G. Liu, A. V. Sumant, V. Goyal, and A. A. Balandin, Nano Lett. **12**(3), 1603–1608 (2012).
[4]Y. Zhu, S. Murali, W. Cai, X. Li, J. W. Suk, J. R. Potts, and R. S. Ruoff, Adv. Mater. **22**(35), 3906–3924 (2010).
[5]L. M. Lawton, N. H. Mahlmeister, I. J. Luxmoore, and G. R. Nash, AIP Adv. **4**(8), 087139 (2014).
[6]C. Lee, X. D. Wei, J. W. Kysar, and J. Hone, Science **321**(5887), 385–388 (2008).
[7]H. Chen, M. B. Müller, K. J. Gilmore, G. G. Wallace, and D. Li, Adv. Mater. **20**(18), 3557–3561 (2008).
[8]M. Zhang, L. Huang, J. Chen, C. Li, and G. Q. Shi, Adv. Mater. **26**(45), 7588–7592 (2014).
[9]D. Yu and L. Dai, Appl. Phys. Lett. **96**(14), 143107 (2010).
[10]S. Lee, J. Oh, R. S. Ruoff, and S. Park, Carbon **50**(3), 1442–1444 (2012).
[11]M. C. Lin, M. Gong, B. Lu, Y. Wu, D. Y. Wang, M. Guan, M. Angell, C. Chen, J. Yang, B. J. Hwang, and H. Dai, Nature **520**(7547), 324–328 (2015).
[12]L. J. Cote, R. Cruz-Silva, and J. X. Huang, J. Am. Chem. Soc. **131**(31), 11027–11032 (2009).
[13]E. Dervishi, Z. R. Li, F. Watanabe, A. Biswas, Y. Xu, A. R. Biris, V. Saini, and A. S. Biris, Chem. Commun. (27), 4061–4063 (2009).
[14]M. Fang, K. G. Wang, H. B. Lu, Y. L. Yang, and S. Nutt, J. Mater. Chem. **20**(10), 1982–1992 (2010).
[15]M. S. Dresselhaus, A. Jorio, M. Hofmann, G. Dresselhaus, and R. Saito, Nano Lett. **10**(3), 751–758 (2010).
[16]B. Jouault, B. Jabakhanji, N. Camara, W. Desrat, A. Tiberj, J. R. Huntzinger, C. Consejo, A. Caboni, P. Godignon, Y. Kopelevich, and J. Camassel, Phys. Rev. B **82**(8), 085438 (2010).
[17]J. A. Leiro, M. H. Heinonen, T. Laiho, and I. G. Batirev, J Electron Spectrosc. **128**(2–3), 205–213 (2003).
[18]G. Gonçalves, P. A. A. P. Marques, A. Barros-Timmons, I. Bdkin, M. K. Singh, N. Emami, and J. Grácio, J. Mater. Chem. **20**(44), 9927 (2010).
[19]Q. Wang, J. Yan, Z. Dong, L. Qu, and Z. Fan, Energy Storage Mater. **1**, 42–50 (2015).
[20]O. C. Compton, D. A. Dikin, K. W. Putz, L. C. Brinson, and S. T. Nguyen, Adv. Mater. **22**(8), 892+ (2010).
[21]A. A. Balandin, Nat. Mater. **10**(8), 569–581 (2011).